DOI: https://doi.org/10.3986/ac.v54i1.14332

KARST ROCK WEATHERING OF THE GREAT PYRAMID OF GIZA

ZAKRASEVANJE KEOPSOVE PIRAMIDE

Martin KNEZ[1, 2, 3], Tadej SLABE[1, 2, 3], Magdy TORAB[4] & Noura FAYAD[5]

Abstract UDC 551.3.053:552.54(620.21/.22)

Martin Knez, Tadej Slabe, Magdy Torab & Noura Fayad: Karst Rock Weathering of the Great Pyramid of Giza

The exposed stone blocks of soft carbonate rock, from which the pyramid is built, quickly develop a distinctive form and rock relief. The outer parts of the blocks are often undercut into overhangs. On their upper parts, a protective crust forms through rock dissolution and rapid recrystallization under the influence of occasional rain and seeping water, shielding the rock from wind erosion and dissolution. This crust, in turn, is dotted by small pits, whose bare surfaces remain exposed to wind erosion, allowing them to expand and grow deeper. In the lower sections, where the rock is fully exposed, wind erosion primarily carves out larger cups and channels. A thin crust may occasionally form over these sections, but tends to flake off quickly. This process suggests rapid karstification and the ongoing disintegration of the stone blocks.

Keywords: carbonate rock, rock relief, complexometry, Great Pyramid of Giza, Egypt.

Izvleček UDK 551.3.053:552.54(620.21/.22)

Martin Knez, Tadej Slabe, Magdy Torab & Noura Fayad: Zakrasevanje Keopsove piramide

Izpostavljeni skalni bloki mehke karbonatne kamnine, iz katerih je piramida, razmeroma hitro pridobijo značilno obliko in skalni relief. Na zunanjih delih so bloki največkrat previsno spodjedeni. Njihov zgornji del, ki ga občasno dosegata dež in polzeča voda, prekriva skorja, ki nastane z raztapljanjem kamnine in hitro rekristalizacijo ter skalo ščiti pred vetrom in šibkim raztapljanjem. Razčlenjen je z vdolbinicami, katerih površina je pogosto gola in zato izpostavljena vetrni eroziji, kar omogoča njihovo rast. V spodnjem delu, kjer je skala gola, v večini primerov povsem prevladujejo skalne oblike, ki jih dolbe vetrna erozija, torej večje vdolbine in žlebovi. Tanka skorja, ki občasno prekrije njihovo površino, se hitro lušči. Sklepamo na hitro zakrasevanje in razpadanje skalnih blokov.

Ključne besede: karbonatna kamnina, skalni relief, kompleksometrija, Keopsova piramida, Egipt.

[1] Research Centre of the Slovenian Academy of Sciences and Arts, Karst Research Institute, Titov trg 2, SI-6230 Postojna, Slovenia, e-mails: knez@zrc-sazu.si, slabe@zrc-sazu.si

[2] UNESCO Chair on Karst Education, University of Nova Gorica, Glavni trg 8, SI-5271 Vipava, Slovenia

[3] Yunnan University International Joint Research Center for Karstology, Xueyun road 5, CN-650223, Kunming, China

[4] Damanhour University, Faculty of Arts, Department of Geography, Abadia, Agricultureroad, EG-5842001 Damanhour, Egypt, e-mail: torab.magdy@gmail.com

[5] University of Nova Gorica, Glavni trg 8, SI-5271 Vipava, Slovenia, PhD student, e-mail: fayyadnoura43@gmail.com

Received/Prejeto: 11. 2. 2025

1. INTRODUCTION

The pyramid is made up by carbonate rocks. The stone blocks (Figure 1) have characteristic shapes, mostly overhanging outer parts, and are heavily dissected. They are dissected by a rock relief that is unique, yet characteristic of such soft carbonate rocks and conditions. Our explanation is aided by findings from researching the rock relief of the karst surface in the area around the Qara and Farafra oases (Egypt). Thus, the karst that forms on such rock and in such an environment facilitates our understanding of the shaping of the karst surface and our assessment of the efficiency of these processes (Knez et al., 2023).

The rock relief of the karst surface generally provides excellent traces of how the three-dimensional karst and karst features (Knez et al., 2003, 2010, 2011; Debevec, 2012; Knez et al., 2012; Al Ketbi et al., 2014; Gutiérrez Domech et al., 2015; Knez et al., 2015, 2017, 2019; Slabe et al., 2016, 2021; Knez et al., 2020, 2023, 2024; Slabe, 2005, 2009; Ruggieri, 2006) have formed and developed; in this regard, the reading of karst rock, surface and caves presents an important approach to studying them comprehensively.

We can also deduce the speed of karstification, which is also causing this famous structure to deteriorate.

The lower layers on the eastern side are part of the karstified Paleogene parent bedrock limestone (sample EGP101, see chapter 3) of this area. The ancient builders also made use of the elevation on the surface during construction (Raynaud et al. 2008; Hemeda & Sonbol, 2020, 5). The rock is hollowed, which is very noticeable (Figure 2).

Floor channels (Ginés et al., 2009) lead from smaller holes, with water from the pyramid flowing along them. The more porous layers are dissected by cups and small holes, apparently subsoil ones (Figure 3). The bottoms of larger holes have been deepened into the subsoil. Channels lead from some of them and continue down the wall (Figure 2). Small cups dissect the surface between them.

The pyramid is 4500 years old. Its surface has been gradually denuded of the stone cladding for at least 1000 years (Emery, 1960), especially after the earthquake in year 1303 (Hemeda & Sombol, 2020, 2), and thus exposed to climatic conditions. However, some hypothesize that the pyramids have been bare all along (Camuffo, 2018).

Figure 1: The Pyramid of Cheops, aka the Great Pyramid.

Figure 2: Limestone bedrock on which the pyramid is built. Width of view is 7 m.

Figure 3: Hollowness of the bedrock limestone. Width of view is 2 m.

The rock of the stone blocks is biomicrite, fine-grained with microfossils (Hemeda & Sonbol, 2020, 11); it is mostly made up of calcite, some iron oxides and quartz, a little dolomite, opaque minerals, and halite (Hemeda & Sonbol, 2020).

The pyramid is located in a semiarid area, with a rainfall of 25 millimetres per year (Hemeda & Sonbol, 2020, 10) and warm winters and hot summers; the predominant winds are the northwesterly and the Khamasin from the southwest with speeds between 7 and 14 km/h. A good study (El-Marsafawy et al., 2019) on the effects of climate change in Egypt also contains data for Giza: January temperatures range from 13 to 19.7 °C with a relative humidity of 58%, while August temperatures range from 22.4 to 36.8 °C (29.1 °C is the mean) with 45% relative humidity. Wind speed reaches 3.5 m/s in winter and 3.7 m/s in summer. The majority of rainfall occurs in winter in the Mediterranean belt (up to 168 mm) (El-Marsafawy et al., 2019).

Rainfall is definitely scarce, since it amounts to *about 55 millimetres per year*. In the wettest years, it has slightly exceeded 100 mm. Occasionally, the area experiences heavy rain (Ogivile-Herald, 2020). In the area of Cairo, the highest monthly rainfall was recorded in

January (24.4 mm). Wind speed is 4–5 m/s in August and 5–6 m/s in January (El-Marsafawy et al., 2019).

Water channels, flood sediments and the remains of vegetation also bear witness to larger amounts of rain and to the consequent flooding of the surface of northern Egypt at the time of the ancient dynasties (Ogivile-Herald, 2020, 7). It is believed that there was lower rainfall along the Upper Nile, which was therefore less water-rich, as the result of changes over the North Atlantic. The low water level in the Nile brought about famine and the decline of ancient kingdoms (Ogivile-Herald, 2020, 22).

The effects of heating from the sun and of cooling down are said to be most pronounced on the western side of the pyramid (Camuffo, 2018, 89). This is corroborated even by the rock that has crumbled into the tiniest pieces (Figures 4, 5).

When studying the weathering of the different carbonate rocks from which the Sphinx is made, researchers pointed out the rock porosity, the crystallization of salt, the impact of thermodynamics, and the growth of cracks (Gauri et al., 1990). Weathering intensifies crystallization pressure due to the dissolution and crystallization of salt in the rock (Gauri et al., 1990, 58). The moisture that condensates during the night causes dissolution, which

Figure 4: Western side of the pyramid.

Figure 5: Disintegration of stone blocks on the western side of the pyramid.

penetrates the rock in the form of capillaries. During the day, as the moisture evaporates, the salt crystals grow and exert pressure (Gauri et al., 1990, 59).

The carbonate rock is shelly, poorly bound, porous, and finely cracked. There are small, centimetre-sized cups in the surface crust of stone blocks (Hemeda & Sonbol, 2020, 11). The carbonate rock is flaking due to the capillary rising of water, while the distinct porosity is causing the crystals to disintegrate (Hemeda & Sonbol, 2020, 11). The crust on the Pyramid of Menkaure is a trace of the distinct alternation of wetting and drying (Hemeda & Sonbol, 2020, 11). High magnifications under a scanning electron microscope reveal a discontinuous crust, large pores, cracks with salt crystals, and the disintegration of crystals (Hemeda & Sonbol, 2020, 14, 15). Hemeda and Sonbol (2020, 21) rate the stability of the stone building blocks as moderate due to the weak binder between the calcite grains.

In the lower part of the Great Pyramid's cross-section, we can also see distinct wind erosion of the rock (Camuffo, 2018, 83).

The majority of relevant studies on this topic serve as a basis for determining the vulnerability of unique cultural heritage sites. The present article marks an important contribution to understanding the weathering of cultural heritage.

2. RESEARCH METHODOLOGY

The subject of the study was the rock relief and the rock features of the Great Pyramid of Giza. After identifying the rock features at the site, we discerned their shape and made thorough descriptions. We linked their formation and shape with geological characteristics. The numerous photographs aided us in further researching the rock features. Next, the identification and description of the examined karst features were combined into a general interpretation of the rock relief. We defined the prevalent factors and the interaction of factors behind the formation of individual rock features. By combining these features into a rock relief, an attempt was made to determine the evolution of stone block shapes.

Nineteen microscopic thin sections were prepared and examined by transmitted light. Prior to the microscopic examination, half of each sample was dyed with alizarin red dye (1,2-dihydroxyanthraquinone, known also as Mordant Red 11; Evamy & Sherman, 1962) to detect calcite. Combining the observations with the results of the complexometric titration analysis, we were able to determine the properties of the rock.

All samples were ground and dried at 105 °C for 24 hours followed by cooling in a desiccator for 30 minutes prior to weighing. We performed 6 complexometric titration analyses on 6 selected rock samples. We used two reference methods, determination of calcium oxide by EGTA and determination of magnesium oxide by DCTA (CEN, 2013). Both methods use photometric determination. The indicator methylthymol blue changes color from pale green to pink in the case of calcium oxide, and from blue to gray in the case of magnesium oxide.

3. ROCK

3.1. MACROSCOPIC DESCRIPTION

We present the descriptions of three different rock samples.

Sample EGP101

The rock presented by sample EGP101 is fine-grained and very porous; on the surface exposed to the atmosphere the rock crumbles to the touch. Well visible on the outer part of the rock, about 3 cm thick, are cracks with a diameter of up to 1 mm; they are mostly distributed along sedimentary laminae, but also often transversally or in directions that are not connected with sedimentation. The inside of the rock, 2 to 3 cm below the surface, is much less flaky and crumbly; there, the clasts are still bound together well.

Rare grey intraclasts are visible in the rock; in some sections, numerous bioclasts are well visible macroscopically, mostly from the genera Nummulites and Operculina (Figure 6).

The clasts in the rock come in different colours: from almost white (White N9) through grey (Light grey N7) to the predominant orange ones (Very pale orange

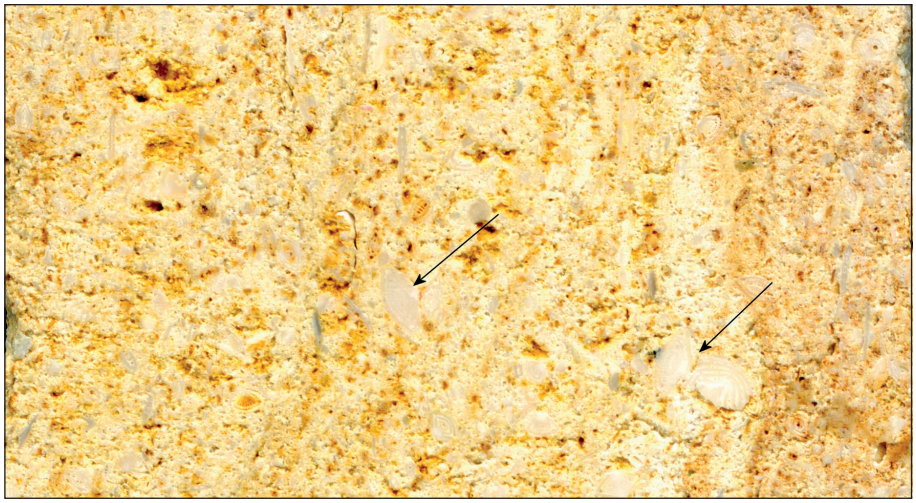

Figure 6: The rock slice of sample EGP101 prepared for thin section. Image width is 4 cm.

10 YR 8/2, Greyish orange 10 YR 7/4, Dark yellowish orange 10 YR 6/6). We have classified the overall colour of the rock as Pale yellowish orange (10 YR 8/6).

This carbonate rock originates from the parent bedrock, forming the lower part of the pyramid -its base. We assume that, at its highest point, it extends upward to an unknown height, forming the core of the pyramid, while at the corners, it transitions into or continues into the surrounding terrain. The contact between the bedrock and the blocks transported from elsewhere was most clearly visible on the eastern face of the pyramid.

Sample EGP102

The rock presented by sample EGP102 is fine-grained and solid; even on the surface exposed to the atmosphere, the rock is not crumbly and is uniform and homogeneous. No bioclasts or other inorganic clasts are macroscopically visible in the rock. No cracks are visible in the rock. In some places on the weathered surface, we can see protruding clusters of dark grey (Greenish grey 5 GY 6/1) spherical mineral grains, measuring on average up to 0.5 mm in diameter (Figure 7). Laterally, such mineral grains are found in smaller numbers or even individually. The predominant colour of the rock is pinkish grey (5 YR 8/1).

After cutting the sample, the facet showed slightly blurred lamination of the rock. Visible parallel to the lamination are around 1 cm long oval darker plasticlasts. Also clearly visible are numerous cross-sections of dark grey spherical mineral grains, which are almost side by side; laterally, their frequency and size vary. They are not present in some parts of the rock.

Sample EGP103

The rock is very fine-grained, homogeneous, uniform and solid; it resembles sample EGP102. However, unlike the other two samples, this rock is undergoing intense weathering on the surface and crumbling. Weathering processes cause thin layers of the rock, a few cm thick, to fall off its surface (surface flaking).

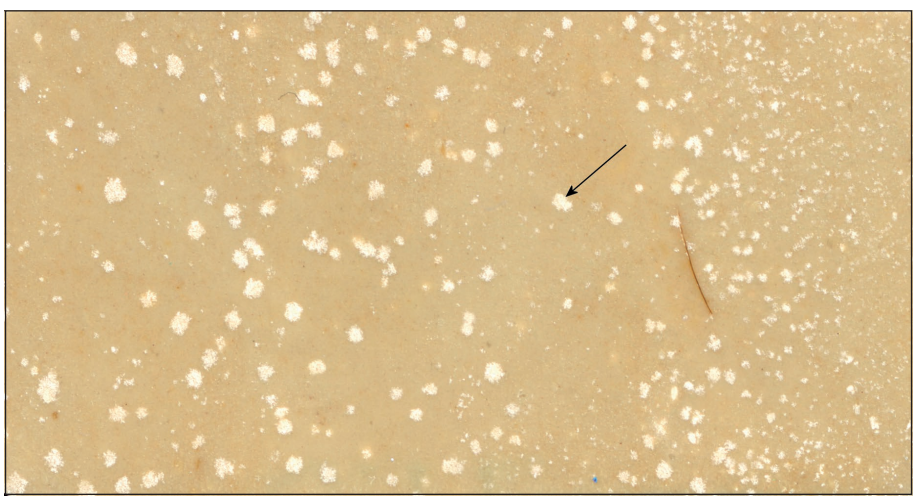

Figure 7: The rock slice of sample EGP102 prepared for thin section. Image width is 4 cm.

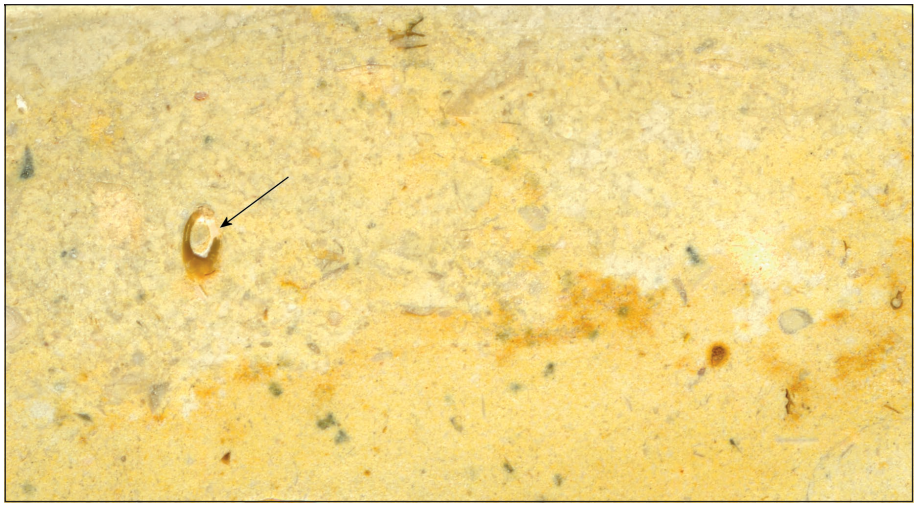

Figure 8: The rock slice of sample EGP103 prepared for thin section; image width is 4 cm.

Visible in the rock are individual spherical unidentifiable bioclasts, mostly measuring up to a few mm in diameter. In addition to bioclasts, we most likely also notice plasticlasts in the rock; these have rather sharp contacts with the predominant rock, only exceptionally does continuously transition into another. Plasticlasts contain numerous dark grey fragments, which most likely belong to different and mostly unidentifiable fragments of bioclasts (Figure 8).

No cracks were detected inside the non-weathered rock.

The colour of the rock changes from white and light grey (White N9 and Very light grey N8) to light orange (Pale yellow orange 10 YR 8/6). The weathered upper or external part of the rock, which is exposed to the atmosphere and on average up to 5 mm thick, ranges in colour from white to grey. Moreover, in some places along tiny cracks the rock has weathered even deeper. In places, the weathered sections reach into the rock in a finger like and meandering way in an irregular pattern and shape; there, they continuously and gradually transition to the non-weathered section.

All three rock samples react intensely to contact with 10% HCl.

The collected rock samples were fragments of stone blocks naturally weathered, which were picked up from the steps.

3.2. MICROSCOPIC DESCRIPTION

We prepared 19 thin sections from three rock samples and examined them in transmitted light. Due to the long-term exposure of the rock to special climate conditions, not all the procedures used in preparing the thin sections were a complete success and had to be repeated. In the concluding phase we selected three thin sections for a thorough microscopic examination.

In the first attempt, we made the thin sections directly from unprocessed rock plates. On account of the considerable porosity, the poorly bound clasts within the rock and most likely also because of the partially weathered rock, in the next phase we reinforced some of the rock plates with Araldite prior to gluing them to the glass slide.

According to the macroscopic results, sample EGP101 presents the rock that is predominant on the outer faces of the pyramid, at least in the lower part.

The rock is enriched by numerous bioclasts, mostly by many whole specimens of the genera Nummulites and Assilinas, and by individual specimens of the genus Operculina (Figure 9). In Ancient Egypt, fossils from the family Nummulitidae that had fallen out of the rock were used as coins or a means of payment (website, 2025); later on, the Latin term *nummulus* meant a small coin and consequently, in addition to the Greek term for money *nomisma*, is the potential origin of the term numismatics, i.e., a branch of history that studies coins. In addition to many whole specimens of the family Nummulitidae, the rock also contains many fragments. The largest nummulite specimens, which are most visible among the fossil remains in the rock and jut out the most from its weathered surface, measure up to 5 mm in diameter. Other, more numerous ones are smaller, with diameters between 0.5 and 1 mm. In some sections of the rock, they are highly prevalent among all the clasts and also touch one another. Together, they take up at least 50% of the rock mass. In terms of frequency, they are followed by Assilinas with much thinner cross-sections, yet some measure over 100 μm in diameter. There are fewer Operculinas in the rock. Besides the described bioclasts, the sample also contains unidentifiable fragments from the group Echinoderms, various foraminifers, and algae. Inorganic grains in the rock include the quite common peloids and micritic and sparry intraclasts of unidentifiable origin and smaller dimensions. The spaces between

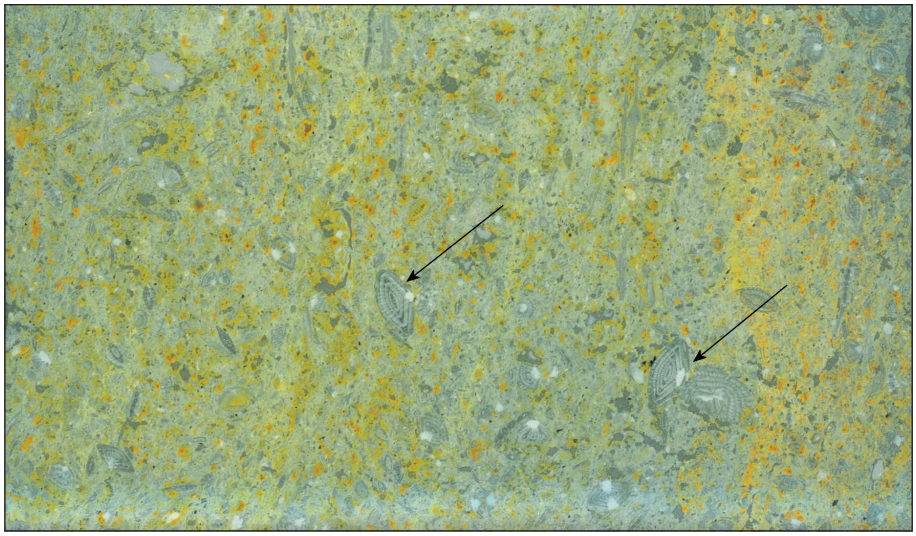

Figure 9: The thin section of rock sample EGP101, impregnated with Araldite; image width is 4 cm.

the numerous and diverse grains are mostly bound by yellowish orange micrite. Sparry cement appears only exceptionally; together with drusy calcite, it fills the rare fenestrae which usually do not measure more than 3 µm in cross-section. Only some grains appear in the rock as dolomitized, most likely as intraclasts (Figure 10). Mechanical compaction is well visible. Porosity is considerable, estimated at around 20%; it also changes laterally within the rock. The voids between the grains are of diverse shapes: from longitudinal ones, measuring over 50 µm in length, through irregularly shaped ones, some with a surface area of over 30x20 µm, to more spherical ones with diameters around 20 µm. The described carbonate rock is biopelintra micrite to microsparite of the packstone to grainstone type of Paleogene age.

The microscopic view of sample EGP102 does not differ much from the macroscopic description. The limestone consists of mostly sparry and microsparitic calcite grains measuring between 0.5 and 1 µm, and comprising at least 85% of the sample. Besides the predominant calcite grains, the microscope slide also contains numerous pellets, all with the uniform diameter of 1 µm. Among the bioclasts we can find up to 10 µm large fragments of and sometimes whole parts of bivalves; in some sections, there are quite numerous uniserial and biserial foraminifers, usually no larger than 5 µm, other unidentifiable whole or broken foraminifers, and individual planktonic foraminifers, most likely from the genera Globigerina and Globotruncana. In the thin sections we can exceptionally also see tiny fragments and in some places even whole gastropods. Various types of cement, e.g., drusy calcite spar or fibrous calcite, are not visible in the rock (Figure 11).

After dyeing the thin section (Figure 12), we discovered that the spherical crystals which are visible macroscopically and within the sawed rock are the beginnings

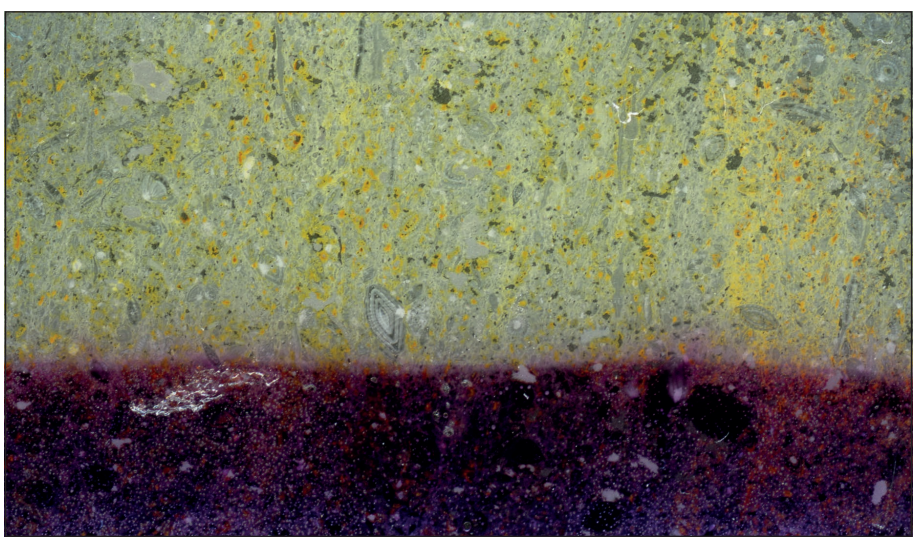

Figure 10: The thin section of rock sample EGP101, impregnated with Araldite and dyed in alizarin red dye; image width is 4 cm.

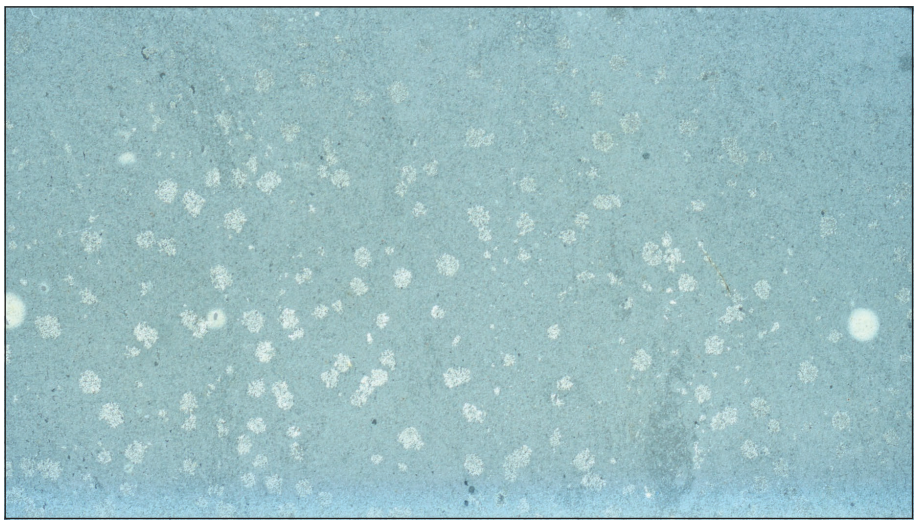

Figure 11: The thin section of rock sample EGP102, impregnated with Araldite; image width is 4 cm.

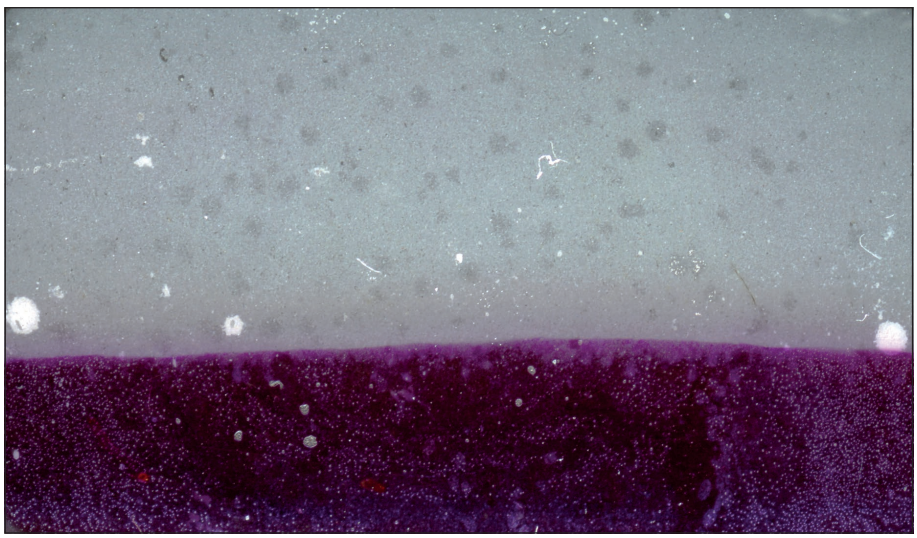

Figure 12: The thin section of rock sample EGP102, impregnated with Araldite and dyed in alizarin red dye; image width is 4 cm.

of dolomitization. The dolomitized fields do not have sharp edges at the contacts with the surrounding rock; in most cases, they transition to the calcite environment partly continuously and partly in an irregular line.

On the whole, the rock has all the characteristics of good mechanical and chemical compaction. Primary porosity is negligible and estimated at less than 3%; the pores are not filled with larger carbonate crystals. No secondary porosity has been detected.

Based on the described characteristics, we have classified the carbonate rock as microsparitic with lateral transitions to microsparitic allochemical limestone of the mudstone or grainstone type.

Sample EGP103 could be described as a transitional rock between samples EGP101 and EGP102 and as the rock on which overhanging crusts are most likely to form. The predominant grains in the rock (Figure 13) are peloids and numerous fragments of mostly unidentifiable bioclasts. The crushed fossil remains indicate considerable transport between the primary habitat and the sedimentation site. Among the crushed fossil fragments, we should mention the many rather large mollusc fragments that measure between 40 and 60 μm along the longer axis and are between 5 and 10 μm thick on average. Most of the larger nummulites are crushed, while the smaller ones, with diameters around 10 μm, also show signs of transport. Also visible among the bioclasts are individual uniserial and biserial foraminifers and a few echinoderms and globigerinas. Micrite binds the clasts in the rock. There are no visible sparite fills between the clasts; drusy calcite spar fills the voids of larger fossils, replacing their original skeleton. Dolomite grains (Figure 14) fill some of the voids in the fossil remains; some of the clasts of unidentifiable origin are dolomite. The rock shows good mechanical compaction; on the other hand, even though it could not be determined macroscopically, it shows considerable primary po-

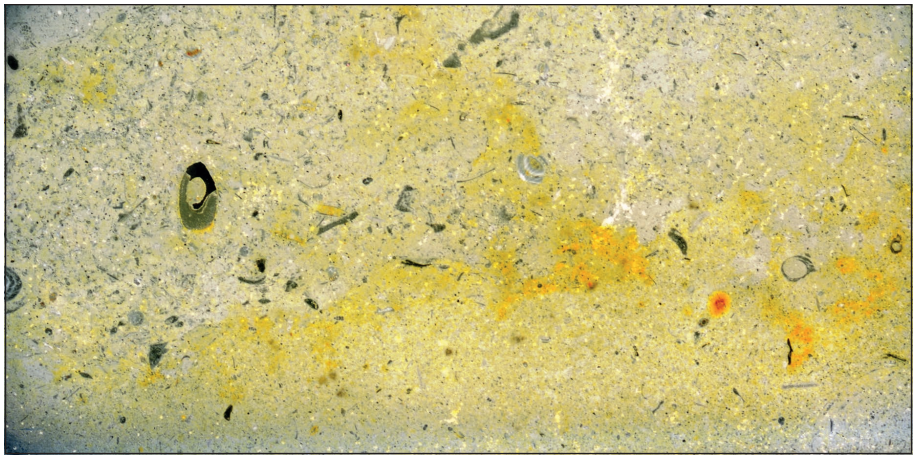

Figure 13: The thin section of rock sample EGP103; image width is 4 cm.

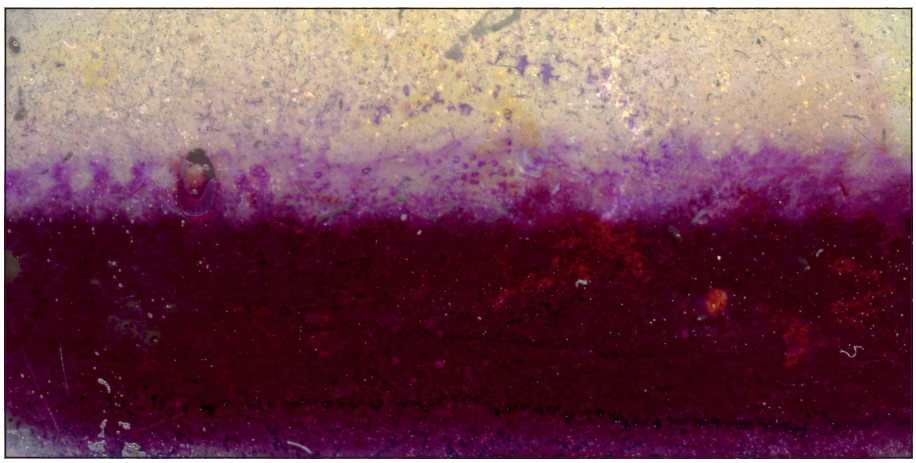

Figure 14: The thin section of rock sample EGP103, dyed in alizarin red dye; image width is 4 cm.

rosity. The latter is estimated in some places at 10 to 20%. Most of the voids are spherical with diameters between 1 and 2 μm, exceptionally between 3 and 7 μm. The rock is pelbiomicrite of the packstone type of Paleogene age.

3.3. COMPLEXOMETRIC TITRATION ANALYSES

All sediment samples (EGP101, EGP102, EGP103) were ground and dried at 105 °C for 24 hours followed by cooling in a desiccator for 30 minutes prior to weighing (Table 1). Using the dissolution method (Engelhardt et al., 1964), we performed 3 complexometric titration analyses on 3 rock samples.

All the samples are very similar to one another. All of them contain roughly between 90 and 93% of calcite, and between 1.1 and 1.7% of dolomite. Sample EGP101 has almost 10% of insoluble residue, sample EGP102 slightly less than 6%, sample EGP103 just under 9%. Total carbonate content in sample EGP102 is just over 94% and in sample EGP103 almost 92%.

Table 1: Complexometric titration analyses of rock samples.

Laboratory designation of the sample	Rock sample	CaO (%)	MgO (%)	Calcite (%)	Dolomite (%)	CaO/MgO	Total carbonate (%)	Insoluble residue (%)
V- 63/23	EGP101	49,77	0,59	88,83	1,23	84,36	90,06	9,94
V- 62/23	EGP102	52,26	0,52	93,27	1,09	100,50	94,36	5,64
V- 64/23	EGP103	50,22	0,83	89,63	1,74	59,79	91,37	8,63

4. ROCK RELIEF OF STONE BLOCKS

The size of stone blocks in the lower part of the pyramid is about 1.5 x 1.5 x 2 metres, and 0.5 x 1 x 1 m in the upper part (Emery, 1960). The bedding planes in the blocks are mostly horizontal. This dictates the development of notches and affects the rock relief.

The characteristic shapes of large stone blocks in the lower part of the pyramid, a few rows above the foundation, and their rock relief (Figure 15) reveal how the pyramid underwent karstification and the latter's development. We can distinguish angular stone blocks (Figure 16) and stone blocks eroded into overhangs (Figures 15, 17, 18), which are especially typical of rapid reshaping. In the upper part covered by crust, the overhanging stone block (Figures 11, 13, 17, 18) is generally densely dissected with cups (Figures 18-arrows, 19). The cups are elongated in the direction of rock stratification and often bound into longitudinal series (Figures 17, 18). They are hemispherical; individual cups are up to one decimetre deep with vaster or asymmetrical interiors, which is dictated by the rock or the most common direction/whirling of the wind. The bottoms of larger cups are covered by sand from the disintegrated rock (Figure 20); in some places, subsoil cups have formed (Slabe & Liu, 2009). Individual stone blocks that are placed vertically to the stratification also contain small elongated cups (Figure 21). Smaller cups dissect the larger ones. The cups have formed where the rock is weak; in this case, mostly due to the discontinuity of the crust and distinct porosity, or are located where a larger segment of the rock has fallen off. The upper parts of the blocks often protrude from the surrounding surface (Figures 15, 22). Their outer walls, which are partly lighter in colour, most often overhang (some very distinctly) or are dissected by larger longitudinal cups and mostly denuded or covered by a thin layer of flaking crust. The reason for this is that the rock is crumbling into tiny pieces (Figures 22, 23).

The creation and shaping of the cups are also affected by fossils, which generally protrude from the

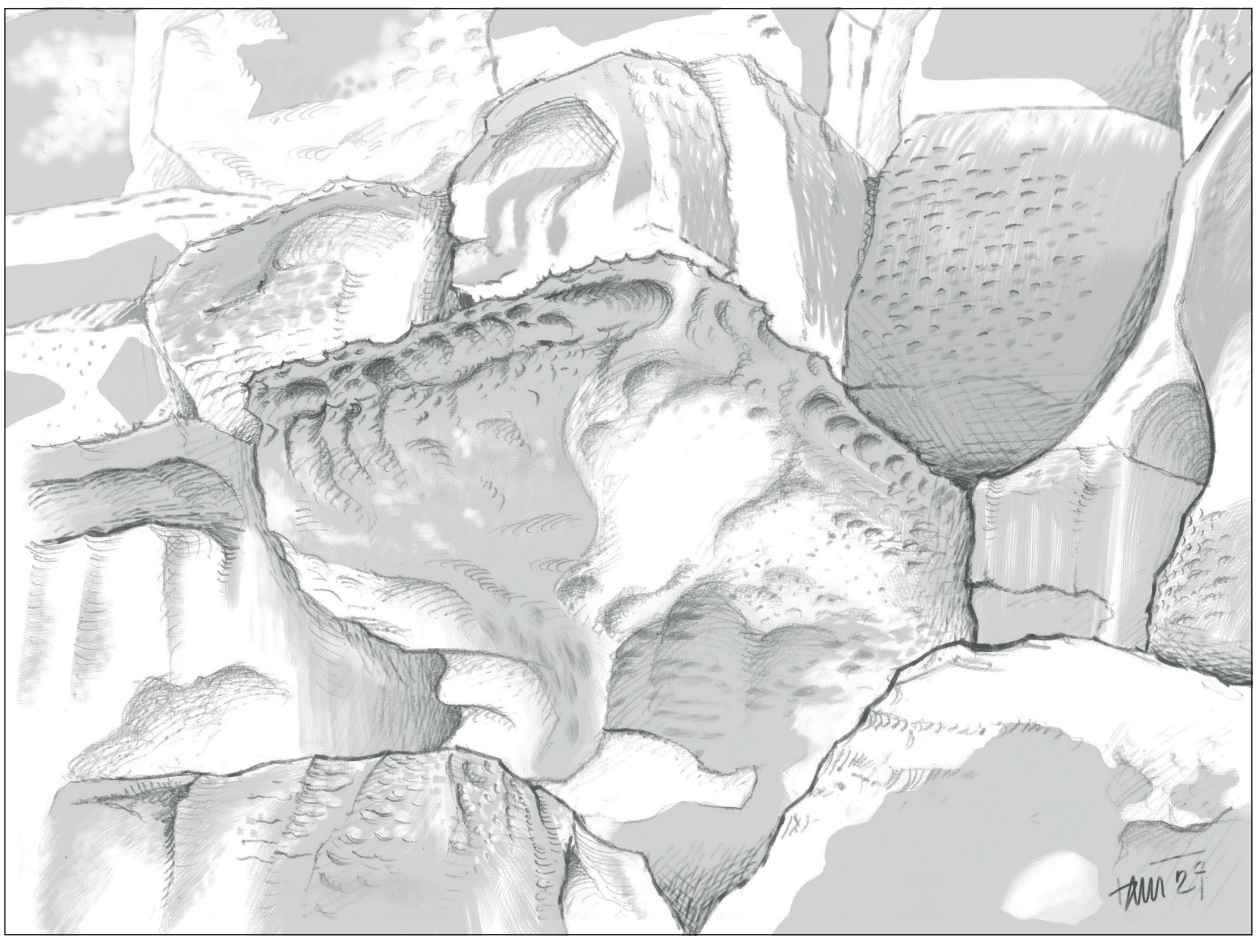

Figure 15: Characteristic shape of a stone block due to karstification and wind erosion. Width of view is 4 m.

Figure 16: Preserved shape of a stone block. Width of view is 4 m.

Figure 17: Eroded stone blocks. Width of view, lower part, is 12 m.

Figure 18: Eroded stone blocks. Width of view is 12 m.

Figure 19: Cups and pits (arrow). Width of view is 1.5 m.

Figure 20: Cups, larger with sand on the bottom. Width of view is 1 m.

Figure 21: Stone block and its relief on vertical stratification. Width of view is 2 m.

Figure 22: Stone blocks with caps. Width of view is 9 m.

Figure 23: Overhanging rock block with crust cap and below wind cups with flaking surface. Width of view is 4 m.

rock surface of the rock that contains them (Figure 24). They are predominant in the bottom layers of the pyramid. The carbonate rock block that mostly contains fossils is more resistant to wind erosion, which is why its walls are usually not eroded into overhangs (Figure 21). However, such blocks are also more distinctly pitted on the tops and exposed parts of the walls, which are being dissolved by water the most. The cups in them

Figure 24. Stone block from a fossil-bearing rock. Width of view is 0.75 m.

Figure 25: Pits in fossiliferous rock. Width of view is 4 m.

are of different sizes, with diameters up to 3 decimetres. (Figure 25).

The surface of the part of the stone block containing the cups is covered with a relatively hard crust in a darker colour. The same applies to the walls situated perpendicularly below the top; the only exception being the lighter bands that are traces of water steadily flowing from the top (Figure 26). The wall ridges exposed

Figure 26: Traces of water runoff from the top of a stone block and wind cups in its lower part. Width of view is 4 m.

Figure 27: Rock ridge with a crust.

to the rain are also covered by crust and are more solid (Figure 27). Therefore, crust forms on surfaces reached by rain or a smaller amount of trickling water. So, similar as tafone shaping (Al Farraj Al Ketbi et al. 2014, 36). Parts of the rock that are not covered by crust, or where the crust on them is flaking off (Figures 15, 26, 28), are weathering faster and being carved out by the wind. This is most noticeable on the walls of blocks below the caps, which are hence most often overhanging. They are dissected by wind cups that are created on bare surfaces between patches of thin wall crusts (Figure 29). Denuded parts of the rock are dissected by larger, in some cases tall, wall cups that notch into the crust at the top (Figures 30, 31); such cups also form at the contacts of stone blocks (Figure 29). In some places, small holes form along the contacts of stone blocks (Figure 32) and

Figure 28: Crust flaking. Width of view is 4 m.

Figure 29: Depressions – traces of wind erosion. Width of view is 8 m.

distinct vertical cracks (Figure 33), and on the walls of larger cups (Figure 34). In other places, the binder between the blocks may protrude from the contact (Figure 35). Only the tops of rare stone blocks are distinctly eroded by wind. Their shapes mostly complement the top blocks that have an eroded lower part. Thus, a channel is formed between two stone blocks, or several of them (Figure 32). The erosion of the middle parts (Figure 35) seems to be dictated by the rock stratification. In some places, we can see artificial longitudinal notches (Figure 36) in stone blocks that are relatively newly denuded. Weathering and wind erosion are also deepening the cups in the crust; their interiors are either denuded or the crust is flaking off their rims in thin layers (Figures 37, 38). Aeolian rock forms (Figure 26) often reveal the prevailing directions of the wind and its cur-

Figure 30: Wind-formed depressions. Width of view is 15 m.

Figure 31: Shallow cups on the ceiling of larger wind-formed recesses. Width of view is 5 m.

Figure 32: Hollows and channels at the contact points of stone blocks. Width of view is 9 m.

Figure 33: Hollow next to a vertical fracture. Width of view is 6 m.

Figure 34: Hollows within depressions. Width of view is 9 m.

Figure 35: Binding material between stone blocks and a recess in the middle of a stone block. Width of view is 4 m.

Figure 36: Artificial recess in the wall of a stone block.

Figure 37: Flaking of cups circumferences. Width of view is 1.5 m.

Figure 38: Flaking of cups circumferences. Width of view is 5 m.

Figure 39: Crust covering bare rock surfaces. Width of view is 3 m.

rents, which are dictated by the shape of the pyramid and of the stone blocks.

In some places, denuded parts of the carbonate rock are predominant (Figure 30). The processes of the dissolution and crusting of the surface and of its denudation are repetitive. Namely, the old crusts are flaking off, while the already denuded parts are once again being covered with a new crust (Figure 39). Only the walls of individual stone blocks are fully shaped by wind erosion. There are also stone blocks whose surfaces are entirely crusted and that have retained their rectangular shape.

These are the most vital processes causing the three-dimensional dissection of the rock and the development of rock relief.

Figure 40: Stratification of the pyramid because of different rock.

Figure 41: Wall channel. Width of view is 3.5 m.

Such karstification and wind erosion processes have also been observed in the area of the Farafra depression (Knez et al., 2023). The crumbling of the porous rock into tiny pieces is preparing it for the more intense process of wind erosion.

Individual stone blocks and in some places whole segments of the pyramid are thoroughly eroded and weathered (Figures 5, 30). This is also influenced by the composition and stability of the rock, which is also reflected in the stratification of the pyramid and in the size of stone blocks (Figure 40).

With regard to crust forms that arise due to the dissolution of the rock and recrystallization, condensation and intense evaporation of moisture also play an important part in the process. A thicker crust forms in places reached by raindrops and trickling water. Wind erosion is usually less effective on such rock surfaces. The darker colour seems to be the result of algae presence in the crust. Perhaps its formation is also aided by the process of crystallization in pores (Gauri et al., 1990), as the rock dissolved by overnight condensation dries up. Only the bands (Figure 16) along which stronger flows of water converge from the top are of a lighter colour. Parts of blocks appear to be covered by calcite and salt, with no cups present. In some places we can make out the beginnings of wall channels (Figure 26) and rarely an actual channel (Figure 41). Thus, the pitted crust is mostly the trace of frequent dissolution of the rock with a small amount of water and crystallization.

The water is indeed dissolving the carbonate rock, however, in this environment the crust is protecting the rock from the most intense processes, such as disintegration and wind erosion.

5. CONCLUSION

The shape of the stone blocks making up the pyramid and their rock relief reveal characteristic weathering and the decisive factors and processes of karstification and wind erosion. There are several intertwining processes at play: first, the less intense dissolution of the rock, which is the result of the small amount of precipitation that directly reaches the rock and of the water trickling down it; second, the rapid evaporation and the consequent formation of crust on the surface of the rock; and third, the relatively intense wind erosion. Water dissolves the rock; as it evaporates, it covers the rock surface with a harder protective crust, while the wind is carving out the bare surfaces by the sand it transports around. The block surfaces are being continuously denuded and crusted, resulting in the formation of small cups. These, in turn, are composite rock forms, as their bare interiors, covered by nothing more than a thin flaking crust, are being carved out by the wind. Meanwhile, the larger cups being notched into the bare rock are entirely aeolian. We can witness a similar shaping of the rock in the natural environment. This leads to the characteristic shape of the stone blocks. Most often the hard, crust-covered top is wider, with overhanging walls beneath it. The blocks made of carbonate rock, which typically contains fossils, display a less dissected rock relief and have preserved their original shape. This holds true especially for the stone blocks that make up the adjacent small pyramid.

The rapid weathering of the stone blocks should also be noted. Have they really become eroded to the point of being bare after only 700 years (Hemeda & Sonbol, 2020)? The soft, mostly sandy carbonate rock would certainly account for that. Today, only the crust covering parts of the rock offers some protection against disintegration and wind erosion.

ACKNOWLEDGEMENTS

The authors acknowledge the financial support from the Slovenian Research Agency (research core funding No. P6-0119 and I0-E017). Research was supported and included in the framework of projects “DEVELOPMENT OF RESEARCH INFRASTRUCTURE FOR THE INTERNATIONAL COMPETITIVENESS OF THE SLOVENIAN RRI SPACE – RI-SI-EPOS” and “DEVELOPMENT OF RESEARCH INFRASTRUCTURE FOR THE INTERNATIONAL COMPETITIVENESS OF THE SLOVENIAN RRI SPACE - RI-SI- LifeWatch”; both operations were co-financed by the Republic of Slovenia, Ministry of Education, Science and Sport and the European Union, and the UNESCO Chair on Karst Education.

REFERENCES

Al Farraj, A., Slabe, T., Knez, M., Gabrovšek, F., Mulec, J., Petrič, M., Zupan Hajna, N., 2014. Karst in Ras Al-Khaimah, northern United Arab Emirates. Acta carsologica, 43(1): 23-41. http://www.dlib.si/details/URN:NBN:SI:DOC-SLRFRQXX, DOI: 10.3986/ac.v43i1.579

Camuffo, D., 2018. A Model Simulation of the Solar Energy Impinging on the Giza Pyramids. Egyptian Journal of Archaelogical and restoration Studies, 8, I, 2, 83-89.

CEN, 2013. Method of testing cement - Part 2: Chemical analysis of cement. European committee for standardization, 83 pp.

Debevec, B., Knez, M., Kranjc, A., Pahor, M., Prelovšek, M., Semeja, A., Slabe, T., 2012. Preliminary study for the adaptation of the "Heaven's Cave" for tourist purposes (Phong Nha-Ke Bang National Park, Vietnam). Acta carsologica, 41(1): 115-127. http://www.dlib.si/details/URN:NBN:SI:doc-E8OEVPIC

El-Marsafawy, S., Bakr, N., Elbana, T., El-Ramady, H., 2019. Climate.- The Soils of Egypt, 69-92, Springer, Cham, https://www.researchgate.net/publication/327141448

Emery, K.O., 1960. Weathering of the Great Pyramid. Journal of Sedimentary Petrology, 30(1): 140-143.

Evamy, B.D., Sherman, D.J., 1962. The application of chemical staining techniques to the study of diagenesis of limestones. Proc. Geol. Soc. London, 1599: 102-103.

Gardner, K.L., 1980. Impregnation technique using colored epoxy to define porosity in petrographic thin sections. Can. J. Earth Sci. Queensland, 17: 1104-1107.

Gauri, K.L., Chowdhury, A.N., Kulshreshtha, N.P., Punuru, A.R., 1990. Geologic Features and Durability of Limestone at Sphinx.- Environ Geol Water Sci,16 (1), 57-62.

Ginés, A., Knez, M., Slabe, T., Dreybrodt, W. (Eds.), 2009. Karst rock features–Karren culpturing. ZRC Publishing, Ljubljana, 561 pp.http://www.dlib.si/details/URN:NBN:SI:doc-E3TEDHCT

Gutiérrez Domech, M.R., Knez, M., Slabe, T., 2015. Felo Pérez Mogote (Viñales, Pinar del Río, Cuba): typical shaping of rock surface below dense tropical vegetation. Actacarsologica. 44(1), 47-57. http://ojs.zrc sazu.si/carsologica/article/view/680/2028, DOI: 10.3986/ac.v44i1.680

Hemeda, S., Sonbol, A., 2020. Sustainability problems of the Giza pyramids.- Heritage Science, Article number 8, https://doi.org/10.1186/s40494-020-0356-9.

Knez, M., Liu, H., Slabe, T., 2010. High Mountain Karren in Northwestern Yunnan, China. Acta carsologica, 39(1): 103-114.

Knez, M., Liu, H. & Slabe, T., 2012. Major stone forest, litomorphogenesis and development of typical shilin (Yunnan, China). Acta carsologica, 41(2/3): 205-218.

Knez, M., Otoničar, B., Slabe T., 2003. Subcutaneous stone forest (Trebnje, Central Slovenija). Acta carsologica, 32(1): 29-38.

Knez, M., Rubinić, J., Slabe, T., Šegina, E., 2015. Karren of the Kamenjak hum (Dalmatian Karst, Croatia): from the initial dissection of flat surfaces by rain to rocky points. Acta carsologica, 44(2): 191-204. http://www.dlib.si/details/URN:NBN:SI:DOC-PUJ5VR8P

Knez, M., Ruggieri, R., Slabe, T., 2019. Karren above Custonaci (Sicily, Italy). In: The European Bi-annual Conference on the Hydrogeology of Karst and Carbonate Reservoirs, Eurokarst, The European Conference on Karst Hydrogeology and Carbonate Reservoirs, Besançon, France, 98 pp.

Knez, M., Slabe, T., Audra, P., 2024. Karren of Provence (France), Gréolières, Caussols, Tourrettes-sur-Loup and Luberon, Acta carsologica, 53(2-3): 145-185. https://ojs.zrc-sazu.si/carsologica/article/view/13889/12264, DOI: 10.3986/ac.v53i2-3.13889

Knez, M., Slabe, T., Panisset Travassos, L.E., 2011. Karren on laminar calcarenitic rock of Lagoa Santa (Minas Gerais, Brazil). Acta carsologica, 40(2): 357-367. http://www.dlib.si/details/URN:NBN:SI:doc-1BRLALPF.

Knez, M., Slabe, T., Torab, M., Fayad, N.H., 2023. Karst rock relief of Qara and White desert (Western desert of Egypt). Acta carsologica, 52(2/3): 197-217. https://ojs.zrc-sazu.si/carsologica/article/view/12796/11894, DOI: 10.3986/ac.v52i2-3.12796

Knez, M., Slabe, T., Trajanova, M., Akimova, T., Kalmykov, I., 2020. The karren peeling off on marbles in Altai (Altai Republic, Russian Federation). Acta carsologica, 49(1): 11-38. http://www.dlib.si/details/URN:NBN:SI:doc-9UMBN4X3, DOI: 10.3986/ac.v49i1.7197

Knez, M., Slabe, T., Urushibara-Yoshino, K., 2017. Lithology, rock relief and karstification of Minamidaito Island (Japan). Acta carsologica, 46(1): 47-62. http://www.dlib.si/details/URN:NBN:SI:DOC-GBB4EVAQ, DOI: 10.3986/ac.v46i1.2022

Ogilvie-Herald, C., 2020. Climate Change and the Age of the Great Sphinx, https://www.academia.edu/resource/work/43952795.

Raynaud S., De la Boisse H., Makroum F. M., Bertho, J.,

2008. Geological and Geomorphological study of original hill at the base of Fourth Dynasty Egyptian monuments, HAL archive, 1-24, https://hal.archives-ouvertes.fr/hal-00319586.

Ruggieri, R., 2006. Egyptian desert karst paleo-morphologies.- Proceedings of the 2nd Middle-East Speleology Symposium, Beirut, 112-116.

Slabe, T., 2005. Two experimental modelings of karst rock relief in plaster: subcutaneous "rock teeth" and "rock peaks" exposed to rain. Zeitschrift für Geomorphologie, 49(1): 107-119.

Slabe, T., 2009. Karren simulation with plaster of Paris models. In: Gines, A., Knez, M.,

Slabe, T., Dreybrodt, W. (Eds.) Karst rock features–Karren sculpturing. ZRC Publishing, pp. 47–54.

Slabe, T., Hada, A., Knez, M., 2016. Laboratory modeling of karst phenomena and their rock relief on plaster, subsoil karren, rain flutes karren and caves. Acta carsologica, 45(2): 187-204. http://www.dlib.si/details/URN:NBN:SI:doc-NFDTIG7J, DOI: 10.3986/ac.v45i2.4623

Slabe, T., Knez, M., Drame, L., 2021. Development model of rock relief on thick horizontal and gently sloping rock strata exposed to rain. Acta carsologica, 508(2/3): 209-230, ilustr. ISSN 0583-6050. https://ojs.zrc sazu.si/carsologica/article/view/ 9308/ 9659, http://www.dlib.si/details/URN:NBN:SI:doc-W7VPJ05Q, DOI: 10.3986/ac.v50i2-3.9308

Slabe, T., Liu, H., 2009. Significant subsoil rock forms. In: Gines, A., Knez, M.,

Slabe, T., Dreybrodt, W. (Eds.) Karst rock features–Karren sculpturing. ZRC Publishing, pp. 123–137. Middle-East Speleology Symposium, Beirut, 112-116. Website, 2025. https://en.wikipedia.org/wiki/Nummulite. [Accessed 26 March 2025]